ADVANCED MATERIALS

[13] T. J. Lenk, D. H. T. Lee, J. T. Koberstein, *Langmuir* **1994**, *10*, 1857.
[14] H. Baltes, M. Schwendler, C. Helm, R. Heger, W. A. Goedel, *Macromolecules* **1997**, *30*, 6633.
[15] One can calculate the thickness of the monolayer before transfer by dividing the surface concentration by the density of the polymer (approx. 1 g/cm^3). In this calculation, it does not matter whether the surface concentration is expressed as chains, repeat units, or mass per area as long as the density is expressed in the equivalent way, i.e., chains, repeat units, or mass per volume, respectively.
[16] M. Antonietti, J. Heyne, H. Sillescu, P. Lindner, *Makromol. Chem.* **1991**, *192*, 3021.
[17] V. Schädler, J. Spickermann, H. J. Räder, U. Wiesner, *Macromolecules* **1996**, *29*, 4865.

Dendrimer-Encapsulated Pt Nanoparticles: Synthesis, Characterization, and Applications to Catalysis**

By *Mingqi Zhao* and *Richard M. Crooks**

In this report we demonstrate a general template-based method for preparing monodisperse platinum nanoparticles suitable for fundamental studies and for use in electrocatalysis. Our approach involves the use of fourth-generation (G4) polyamidoamine (PAMAM) Starburst dendrimers[1] as both template and stabilizer. These dendrimers are monodisperse, hyperbranched polymers, which are roughly spherical in shape, highly functionalized, sterically crowded on the exterior, and somewhat hollow in the interior. The cavities inside a dendrimer have shown their ability to trap guest molecules.[2–4] We,[5] and others,[6,7] have found that transition-metal ions, including Cu^{2+}, Ag^{+}, Pt^{2+}, Pd^{2+}, Ru^{3+}, and Ni^{2+}, partition into the interior of PAMAM dendrimers, where they are strongly complexed by interior functional groups. The number of complexed metal ions per dendrimer can be nearly monodisperse.[5] Thus, by preloading a dendrimer "nanotemplate" with suitable metal ions and then chemically reducing this composite in situ, a dendrimer-encapsulated metal cluster results (Fig. 1). Here, we show that between 12 and 60 Pt^{2+} ions can be loaded into a hydroxyl-terminated G4 PAMAM dendrimer (G4–OH), and that upon reduction with BH_4^- an entrapped cluster containing the same number of atoms results. The dendrimer stabilizes the metal cluster by preventing agglomeration; however, it does not fully passivate the metal surface and therefore the sequestered cluster can be used for electrocatalytic reduction of O_2.

[*] Prof. R. M. Crooks, M. Zhao
Department of Chemistry
Texas A&M University
PO Box 30012
College Station, TX 77842-3012 (USA)

[**] This work is supported by the National Science Foundation (CHE-931344) and the Robert A. Welch Foundation. M.Z. acknowledges an Electrochemical Society Summer Fellowship. We thank Mr. Mark Kaiser (Dendritech, Inc., Midland, MI) for providing technical information and supplying some of the Starburst PAMAM dendrimers used in this study. TEM results are based upon research conducted at the Transmission Electron Microscopy Laboratory in the Department of Earth and Planetary Science of the University of New Mexico, which is supported by NSF, NASA, and the State of New Mexico.

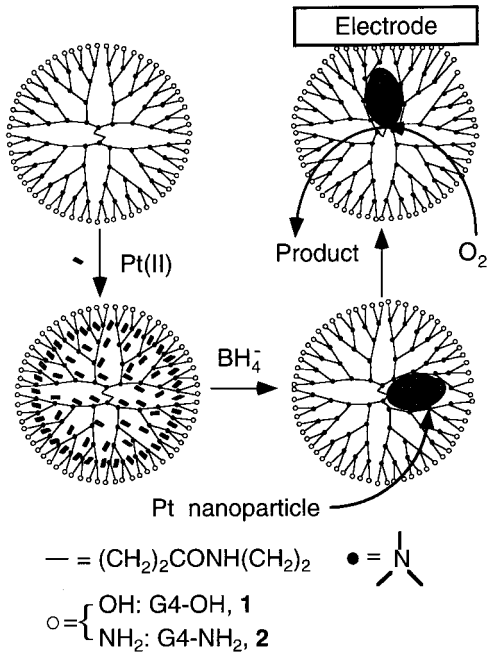

Fig. 1. Schematic illustration of fourth-generation (G4) PAMAM dendrimers having –OH and NH_2 terminal groups, synthesis of Pt nanoparticles within the hydroxyl-terminated dendrimer template, and attachment of the composite to an electrode surface. Between 12 and 60 Pt^{2+} ions can be loaded into a single dendrimer and, upon reduction with BH_4^-, an entrapped cluster containing the same number of atoms results. The dendrimer-encapsulated Pt nanoparticles are electrocatalytically active.

Noble-metal nanoparticles are of fundamental interest and technological importance because of their applications as catalysts.[8–12] Synthetic routes to metal nanoparticles include evaporation and condensation, and chemical or electrochemical reduction of metal salts in the presence of stabilizers.[8,9,13–15] The purpose of the stabilizers, which include polymers, ligands, and surfactants, is to control particle size and prevent agglomeration. However, stabilizers also passivate cluster surfaces. For some purposes, such as catalysis, it is desirable to prepare small, stable, but not fully passivated, particles so that substrates can access the encapsulated clusters. Another promising method for preparing clusters and colloids involves the use of templates, such as reverse micelles[16,17] and porous membranes.[11,18,19] However, even this approach results in passivated, or at least mostly passivated, nanoparticles unless the template is removed. Removal of the template may result in slow agglomeration of the naked particles. By using dendrimers as both monodisperse templates and stabilizers, we achieve particle stability and full control over particle size, while simultaneously allowing substrates to penetrate the dendrimer interior and access the cluster surface. To the best of our knowledge this advantageous set of properties is unique.

Our approach for depositing Pt nanoparticles inside dendrimers is simple. First, a predetermined amount of Pt^{2+} is sorbed into dendrimer **1** (G4–OH, Fig. 1). Second, the encapsulated ions are reduced with BH_4^- to yield the dendri-

  0935-9648/99/0302-0217 $ 17.50+.50/0

mer-encapsulated nanoparticle. Figure 2a provides spectroscopic evidence for Pt^{2+} sorption into G4–OH. In the absence of the dendrimer, the spectrum of a freshly prepared solution of 3 mM $PtCl_4^{2-}$ consists of a strong absorption peak at 216 nm arising from a ligand-to-metal charge-transfer (LMCT) transition.[20] When 0.05 mM G4–OH is added to this solution, a new band at 250 nm emerges while the band at 216 nm decreases and shifts slightly to 219 nm. The isosbestic point at 234 nm suggests replacement of $PtCl_4^{2-}$ chlorine ligands with tertiary amine ligands from the dendrimer interior (see below). This ligand-exchange reaction is slow, which is consistent with previous observations for other Pt^{2+} complexes.[21] The absorbance at 250 nm is proportional to the number of Pt^{2+} ions in the dendrimer over the range 0–60 (G4–OH$(Pt^{2+})_n$, n = 0 to 60), which indicates that it is possible to control the G4–OH/Pt^{2+} ratio.

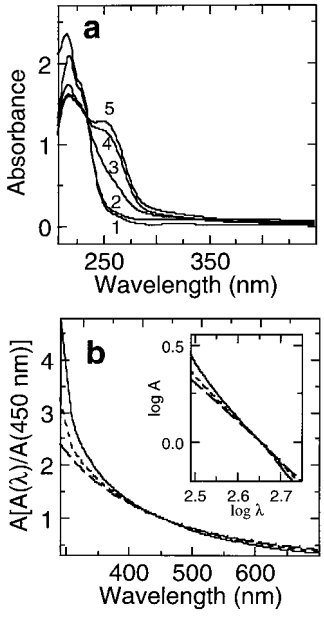

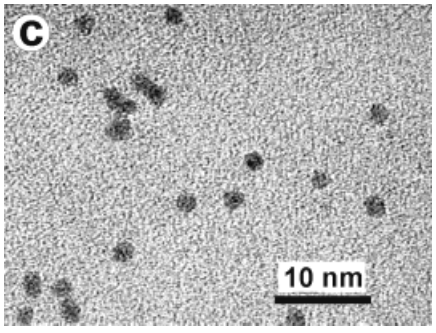

Fig. 2. UV-vis spectroscopy and HRTEM data demonstrating sorption of Pt^{2+} ions into G4–OH dendrimers and subsequent chemical reduction to yield dendrimer-encapsulated platinum metal clusters. a) Time-dependent UV-vis spectroscopic data obtained after mixing 3 mM $PtCl_4^{2-}$ and 0.05 mM G4–OH. Curves 1–5 correspond to 0, 1, 7, 26, and 45 h after mixing. b) UV-vis spectra of solutions containing G4–OH(Pt_{12}) (solid line), G4–OH(Pt_{40}) (short dashes) and G4–OH(Pt_{60}) (longer dashes) normalized to A = 1 at λ = 450 nm. Logarithmic plots of these data, shown in the inset, demonstrate that larger particles result in less negative slopes. The optical path length for all UV-vis measurements was 0.1 cm. c) HRTEM image of G4–OH(Pt_{60}), showing the monodisperse size and shape distribution.

Control experiments confirm that the Pt^{2+} ions are inside the dendrimer rather than complexed to the exterior hydroxyl groups. For example, when a 0.05 mM solution of dendrimer **2** (100 % NH_2 terminal groups) is added to a 3 mM $PtCl_4^{2-}$ solution an emulsion, and then precipitation, results. This is a consequence of Pt^{2+}-induced crosslinking of the NH_2-functionalized dendrimers,[22] which does not occur with the non-complexing OH-terminated materials. Additionally, when an acidified 0.05 mM G4–OH solution (pH 1) is added to a 3 mM $PtCl_4^{2-}$ solution, no spectral changes occur, indicating that protonated interior tertiary amines do not complex Pt^{2+} under these conditions. Finally, X-ray photoelectron spectroscopy (XPS) of G4–OH$(Pt^{2+})_{60}$ indicates that the ratio of Pt to Cl is 1/3, which suggests that complexation of $PtCl_4^{2-}$ to the dendrimer is accompanied by loss of one chlorine ligand from the Pt complex. Taken together these three results suggest that up to 60 Pt^{2+} ions are complexed within G4–OH via Pt^{2+}–amine interactions.

Chemical reduction of an aqueous solution of G4–OH$(Pt^{2+})_n$, n = 12, 40, and 60, yields intradendrimer platinum metal nanoparticles (G4–OH(Pt_n)). Spectra of these materials are shown in Figure 2b; they display the monotonic increase in absorbance typical of the interband transition of Pt nanoparticles.[23,24] Control experiments clearly demonstrate that the Pt clusters are sequestered within the G4–OH dendrimer. For example, BH_4^- reduction of the previously described G4–$NH_2(Pt^{2+})_n$ emulsions results in immediate precipitation of large Pt clusters. After filtration of the sample with a 0.2 μm PTFE (polytetrafluoroethylene) filter, absorbance spectra indicate almost no interband transition for the reduced G4–$NH_2(Pt^{2+})_n$ solution. This shows that Pt particles arising from Pt^{2+} ions bound to terminal primary amine ligands agglomerate and only the intradendrimer-bound Pt^{2+} ions yield stable, soluble clusters. Importantly, the dendrimer-encapsulated particles do not agglomerate for up to 150 days and they redissolve in solvent after repeated dryings.

The absorbance intensity in Figure 2b is related to the particle size. A plot of $\log A$ versus $\log \lambda$ provides qualitative information about particle size: the negative slopes are known to decrease with increasing particle size.[24] For aqueous solutions of G4–OH(Pt_{12}), G4–OH(Pt_{40}), and G4–OH(Pt_{60}), the slopes are –2.7, –2.2, and –1.9, respectively (Fig. 2b, inset). Thus the size of the intradendrimer particles increases with increasing Pt^{2+} loading.

We investigated the dimensions of Pt nanoparticles using a JEOL 2010 high-resolution transmission electron microscope (HRTEM) having a point-to-point resolution of 0.19 nm. A drop of dilute, aqueous G4–OH(Pt_{60}) solution was placed on a copper TEM grid completely covered with carbon and the water was allowed to evaporate. Images were recorded digitally using a charge-coupled device (CCD) camera. The HRTEM image in Figure 2c reveals the spherical shape (at this resolution) and high degree of monodispersity of the Pt clusters. Analysis of 100 randomly

  0935-9648/99/0302-0218 $ 17.50+.50/0

ADVANCED MATERIALS

selected particles indicates their average diameter is 1.6 ± 0.2 nm, which is little larger than the theoretical value of 1.2 nm calculated by assuming the Pt atoms are encompassed within the smallest sphere containing a 60-atom face-centered cubic (fcc) crystal. In a different experiment we imaged monodisperse G4–OH(Pt_{40}) particles, which have a diameter of 1.4 ± 0.3 nm. Pt nanoparticles usually have irregular shapes and a large size distribution when prepared in aqueous solution.[13,25] The observation of very small, predominantly spherical particles in this study may be a consequence of the dendrimer cavity; i.e., the template in which they are prepared. X-ray energy dispersive spectroscopy (EDS) was also carried out, and it unambiguously identifies the particle composition as platinum.

Dendrimers containing Pt^{2+} or platinum-metal nanoparticles are easily attached to Au and other surfaces by immersion in a dilute aqueous solution of the composite for 20 h, followed by careful rinsing and drying.[26,27] Fourier transform infrared–external reflection spectroscopic data of a substrate prepared in this way exhibit peaks at 1665 and 1555 cm^{-1}, characteristic of the high density of amide bonds present within the PAMAM dendrimers. XPS provides elemental compositional information about the modified substrates. For example, the Pt($4f_{7/2}$) and Pt($4f_{5/2}$) peaks are present at 72.8 and 75.7 eV, respectively, prior to reduction, but after reduction they shift to 71.3 and 74.4 eV, respectively, which is consistent with the change in oxidation state from +2 to 0 (Fig. 3).[28] Importantly, XPS data also indicate the presence of chlorine prior to reduction, but it is not detectable from the spectrum of G4–OH(Pt_{60})-modified surfaces.

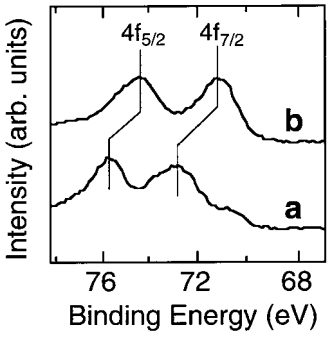

Fig. 3. XPS spectra of G4–OH(Pt^{2+})$_{60}$ before (curve a) and after (curve b) reduction. The shifts of Pt($4f_{7/2}$) from 72.8 to 71.3 eV and Pt($4f_{5/2}$) from 75.7 to 74.4 eV indicate the reduction of interior Pt^{2+}. The XPS peak positions were referenced to the Au($4f_{7/2}$) peak at 83.8 eV and the photoelectrons were detected at a 45° take-off angle.

Pt is the most effective practical catalyst known for O_2 reduction, which is an important electrode reaction in fuel cells.[6] To achieve efficient utilization of Pt in such applications, a large amount of work has been devoted to developing methods for fabricating very small, stable, O_2-accessible clusters. Because our composites appear likely to exhibit all these properties, we thought it reasonable to test them as O_2 reduction catalysts. Figure 4 shows cyclic voltammograms (CVs) of Au/G4–OH(Pt_{60}) in the presence and absence of O_2 and Au/G4–OH in the presence of O_2. In the presence of O_2, the Au/G4–OH-modified electrode yields a relatively small current having a peak potential (E_p) negative of –150 mV. However, when a Au/G4–OH(Pt_{60})-modified electrode is used in the same solution, a much larger catalytic current is observed and the peak potential shifts to the positive value of 75 mV, indicating a substantial catalytic effect. In the absence of O_2, only a small background current is observed for this electrode, confirming that the process giving rise to the peak is O_2 reduction. Importantly, these results conclusively demonstrate that the surface of the dendrimer-encapsulated Pt nanoparticles are accessible to reactants in the solution and can exchange electrons with the underlying electrode surface.

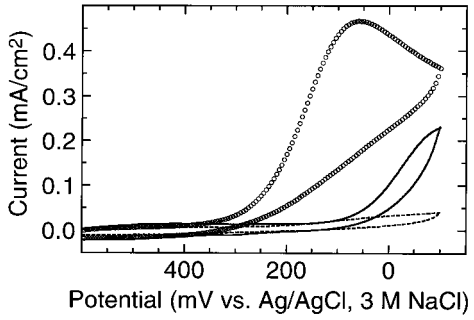

Fig. 4. Cyclic voltammograms of Au electrodes coated with G4–OH in O_2-saturated 1 M H_2SO_4 (solid line) or coated with G4–OH(Pt_{60}) in N_2-(dashed line) or O_2- (circles) saturated 1 M H_2SO_4. Catalytic reduction of O_2 is observed only on the Au/G4–OH(Pt_{60}) electrode. Electrode area: 0.086 cm^2, scan rate: 50 mV/s.

In summary, we have reported three important discoveries. First, dendrimers act as templates for preparing monodisperse precious-metal nanoclusters. Second, dendrimers prevent agglomeration of the nanoclusters by constraining them within their interiors. Third, the dendrimer terminal groups act as a chemical handle, which facilitates surface immobilization. We have taken advantage of all these factors to show that dendrimer/nanocluster composites confined to electrode surfaces act as electrocatalysts for O_2 reduction. Somewhat surprisingly, the Pt nanoclusters communicate electrically with the electrode without the need for mediators, even though the two are probably not in intimate contact. The size of the nanoclusters prepared in this manner depends on the type and generation of the dendrimer used as the template, and also on the number of metal ions preloaded into the dendrimer/template interior prior to reduction. Additional results (not described in this report) indicate that metal clusters can be prepared from many different types of transition-metal ions, and also that it is possible to make bimetallic clusters by sequential loading and reduction of two different metal ions or by co-complexation of two metal ions followed by reduction. We believe this is a very general approach to the preparation of monodisperse metal and semiconductor nanoclusters that will find many applications in fundamental and applied science and technology.

Received: October 8, 1998

  0935-9648/99/0302-0219 $ 17.50+.50/0

[1] F. Zeng, S. C. Zimmerman, *Chem. Rev.* **1997**, *97*, 1681.
[2] J. F. G. A. Jansen, E. E. M. de Brabander-van den Berg, E. W. Meijer, *Science* **1994**, *266*, 1226.
[3] J. F. G. A. Jansen, E. W. Meijer, *J. Am. Chem. Soc.* **1995**, *117*, 4417.
[4] A. I. Cooper, J. D. Londono, G. Wignall, J. B. McClain, E. T. Samulski, J. S. Lin, A. Dobrynin, M. Rubinstein, A. L. C. Burke, J. M. J. Fréchet, J. M. DeSimone, *Nature* **1997**, *389*, 368.
[5] M. Zhao, L. Sun, R. M. Crooks, *J. Am. Chem. Soc.* **1998**, *120*, 4877.
[6] L. Balogh, D. A. Tomalia, *J. Am. Chem. Soc.* **1998**, *120*, 7355.
[7] M. F. Ottaviani, F. Montalti, N. J. Turro, D. A. Tomalia, *J. Phys. Chem. B* **1997**, *101*, 158.
[8] L. N. Lewis, *Chem. Rev.* **1993**, *93*, 2693.
[9] J. S. Bradley, in *Clusters and Colloids* (Ed: G. Schmid), VCH, Weinheim **1994**.
[10] G. J. K. Acres, G. A. Hards, *Philos. Trans. R. Soc. London A.* **1996**, *354*, 1671.
[11] G. L. Che, B. B. Lakshmi, E. R. Fisher, C. R. Martin, *Nature* **1998**, *393*, 346.
[12] E. Reddington, A. Sapienza, B. Gurau, R. Viswanathan, S. Sarangapani, E. S. Smotkin, T. E. Mallouk, *Science* **1998**, *280*, 1735.
[13] G. Schmid, *Chem. Rev.* **1992**, *92*, 1709.
[14] J. D. Aiken III, Y. Lin, R. G. Finke, *J. Mol. Catal. A: Chem.* **1996**, *114*, 29.
[15] M. T. Reetz, W. Helbig, *J. Am. Chem. Soc.* **1994**, *116*, 7401.
[16] C. Petit, P. Lixon, M. Pileni, *J. Phys. Chem.* **1993**, *97*, 12 974.
[17] C. B. Murray, D. J. Norris, M. G. Bawendi, *J. Am. Chem. Soc.* **1993**, *115*, 8706.
[18] C. R. Martin, *Science* **1994**, *266*, 1961.
[19] Y. Zhang, N. Raman, J. K. Bailey, C. J. Brinker, R. M. Crooks, *J. Phys. Chem.* **1992**, *96*, 9098.
[20] M. Gerloch, E. C. Constable, *Transition Metal Chemistry: The Valence Shell in d-Block Chemistry*, VCH, Weinheim **1994**.
[21] F. Fanizzi, F. P. Intini, L. Maresca, G. Natile, *J. Chem. Soc., Dalton Trans.* **1990**, 199.
[22] S. Watanabe, S. L. Regen, *J. Am. Chem. Soc.* **1994**, *116*, 8855.
[23] U. Kreibig, M. Vollmer, *Optical Properties of Metal Clusters*, Springer, Berlin **1995**.
[24] D. N. Furlong, A. Launikonis, W. H. F. Sasse, *J. Chem. Soc., Faraday Trans. 1* **1984**, *80*, 571.
[25] T. S. Ahmadi, Z. L. Wang, T. C. Green, A. Henglein, M. A. El-Sayed, *Science* **1996**, *272*, 1924.
[26] M. Zhao, H. Tokuhisa, R. M. Crooks, *Angew. Chem. Int. Ed. Engl.* **1997**, *36*, 2596.
[27] H. Tokuhisa, M. Zhao, L. A. Baker, V. T. Phan, D. L. Dermody, M. E. Garcia, R. F. Peez, R. M. Crooks, T. M. Mayer, *J. Am. Chem. Soc.* **1998**, *120*, 4492.
[28] C. D. Wagner, W. M. Riggs, L. E. Davis, J. F. Moulder, *Handbook of X-Ray Photoelectron Spectroscopy*, Perkin-Elmer, Eden Prairie **1979**.

CdTe Quantum Dots Obtained by Using Colloidal Self-Assemblies as Templates

By *Dorothée Ingert*, *Nicholas Feltin*, *Laurent Levy*, *Pierre Gouzerh*, and *Marie-Paule Pileni**

Nanometer-size crystals exhibit behavior intermediate between bulk material and molecules. Their sizes range from smaller than to a few times the size of the effective Bohr diameter of an exciton in a bulk crystal. These systems have attracted special attention because of their unique size-dependent properties, including optical properties such as absorption and third-order nonlinearity as well as conversion of solar energy. Since the size dependence of the band levels of semiconductor particles results in a shift of the optical spectrum, quantum mechanical descriptions of the shift have been worked out by several researchers.[1–16]

An important II–VI semiconductor quantum dot is CdTe because of its large exciton Bohr diameter (15 nm). It has received much attention and its bandgap shift with cluster size has been well mapped.[17–25] Usually CdTe quantum dots are made by radio frequency (rf) magnetron sputtering in a glass matrix.[17–25] This communication describes, for the first time, CdTe synthesis by soft chemistry. It is shown that the optical properties of CdTe quantum dots differ markedly with the preparation mode.

The synthesis by soft chemistry first requires disodium telluride, Na_2Te, to be made. Note: This product is highly poisonous and oxidizable. To make Na_2Te we tried two procedures described in the literature.[26] The difference between the two lies mainly in the reaction time and in the amount of naphthalene used as catalyst. However, one procedure gives disodium telluride containing large amounts of impurities; the only procedure suitable for making pure Na_2Te is that described in the Experimental section.

The synthesis of CdTe is performed using water-in-oil droplets, usually called reverse micelles, as templates and is described in detail in the Experimental section. The difference between procedures I and II is that the nanocrystals of CdTe were aged in the micellar solution in procedure I but not in procedure II. The final coated particles are stable in air in powder form.

The particle size, determined from transmission electron microscopy (TEM) images,[27] was controlled by the size of the water droplets in which syntheses were carried out. Similar behavior has been observed for various nanoparticles.[28] As expected, the aging of particles (procedure II) induced an increase in the particle size compared to that observed with procedure I. Table 1 gives the average size of the particles and the size distribution for the two procedures used. Hence procedure I permits a change in the particle size from 2.6 to 3.4 nm, whereas by procedure II it ranges from 3.4 to 4.1 nm. Electron diffraction[27] studies confirmed that the CdTe nanocrystallites exhibited the bulk-like zinc blende crystal structure.[29] The coated particles were analyzed by energy dispersion spectroscopy (EDS);[30] they are composed of 51 % Cd and 49 % Te. The electron diffraction, the energy dispersion spectroscopy, and the average size distribution (13 %) (Table 1) remained unchanged with the two procedures used and for various particle sizes.

As observed for direct semiconductors, the CdTe absorption spectrum[31] is size dependent. A red shift in the ab-

[*] Prof. M. P. Pileni, Dr. D. Ingert, Dr. N. Feltin, Dr. L. Levy
Laboratoire Structure et Réactivité des Systèmes Interfaciaux
URA CNRS 1662, Université Pierre et Marie Curie (Paris VI)
BP 52, 4 Place Jussieu, F-75231 Paris Cedex 05 (France)
and
CEA-CE Saclay, DRECAM-SCM
F-91191 Gif sur Yvette Cedex (France)
Prof. P. Gouzerh
Laboratoire de Chimie des Métaux de Transition, URA-CNRS 419
Université Pierre et Marie Curie (Paris VI)
BP 42, 4 place Jussieu, F-75231 Paris Cedex 05 (France)

  0935-9648/99/0302-0220 $ 17.50+.50/0